

Analysis of Kinetics of Dihydroethidium Fluorescence with Superoxide Using Xanthine Oxidase and Hypoxanthine Assay

JUAN CHEN,¹ STEVEN C. ROGERS,² and MAHENDRA KAVDIA¹

¹Department of Biomedical Engineering, Wayne State University, 2152 Engineering Bldg, 5050 Anthony Wayne Dr., Detroit, MI 48202, USA; and ²Cell and Molecular Biology Program, University of Arkansas, Fayetteville, AR 72701, USA

(Received 15 June 2012; accepted 30 August 2012; published online 11 September 2012)

Associate Editor Gerald Saidel oversaw the review of this article.

Abstract—Superoxide (O_2^-) is an important reactive oxygen species (ROS), and has an essential role in physiology and pathophysiology. An accurate detection of O_2^- is needed to better understand numerous vascular pathologies. In this study, we performed a mechanistic study by using the xanthine oxidase (XOD)/hypoxanthine (HX) assay for O_2^- generation and a O_2^- sensitive fluorescent dye dihydroethidium (DHE) for O_2^- measurement. To quantify O_2^- and DHE interactions, we measured fluorescence using a microplate reader. We conducted a detailed reaction kinetic analysis for DHE- O_2^- interaction to understand the effect of O_2^- self-dismutation and to quantify DHE- O_2^- reaction rate. Fluorescence of DHE and 2-hydroethidium (EOH), a product of DHE and O_2^- interaction, were dependent on reaction conditions. Kinetic analysis resulted in a reaction rate constant of $2.169 \pm 0.059 \times 10^3 M^{-1} s^{-1}$ for DHE- O_2^- reaction that is $\sim 100\times$ slower than the reported value of $2.6 \pm 0.6 \times 10^5 M^{-1} s^{-1}$. In addition, the O_2^- self-dismutation has significant effect on DHE- O_2^- interaction. A slower reaction rate of DHE with O_2^- is more reasonable for O_2^- measurements. In this manner, the DHE is not competing with superoxide dismutase and NO for O_2^- . Results suggest that an accurate measurement of O_2^- production rate may be difficult due to competitive interference for many factors; however O_2^- concentration may be quantified.

Keywords—DHE, Reaction rate constant, Kinetic analysis, Oxidative stress, Cytochrome c.

ABBREVIATIONS

DHE Dihydroethidium
E⁺ Ethidium

EOH 2-Hydroethidium
GSH Glutathione
H₂DCF-DA Dichlorodihydrofluorescein-diacetate
H₂O₂ Hydrogen peroxide
HPLC High performance liquid chromatography
HX Hypoxanthine
MS Mass spectrometry
NO Nitric oxide
O₂⁻ Superoxide
·OH Hydroxyl radical
ONOO⁻ Peroxynitrite
PBS Phosphate buffer solution
ROS Reactive oxygen species
RNS Reactive nitrogen species
SOD Superoxide dismutase
XOD Xanthine oxidase

INTRODUCTION

Superoxide (O_2^-), which is one of the major reactive oxygen species (ROS), is one-electron reduction product of molecular oxygen. O_2^- participates in signaling pathways^{4,9,12} and is a common marker for oxidative stress. O_2^- leads to the formation of other ROS including hydrogen peroxide (H_2O_2), and hydroxyl radical ($\cdot OH$), and reactive nitrogen species (RNS).^{7,22,25} The accurate detection of O_2^- levels is critical for understanding numerous physiological phenomenon and pathologies such as cell proliferation, apoptosis, cardiovascular disease, diabetes and cancer.^{8,15,26,30}

In the previous literature, several methods have been described to detect O_2^- . These methods include lucigenin and luminol assays, electron paramagnetic resonance, high performance liquid chromatography

Address correspondence to Mahendra Kavdia, Department of Biomedical Engineering, Wayne State University, 2152 Engineering Bldg, 5050 Anthony Wayne Dr., Detroit, MI 48202, USA. Electronic mail: kavdia@wayne.edu

(HPLC) coupled with mass spectrometry (MS), and fluorescence.^{7,8,30,32} Most of these methods are not specific for O_2^- detection. For example, lucigenin and dichlorodihydrofluorescein-diacetate ($H_2DCF-DA$) can generate O_2^- and react with other oxidative stress. In addition, some methods can be very harmful to the human biological system. For example, lucigenin can stimulate oxidative stress formation to inhibit endothelium-dependent relaxation,²⁹ and hydroethidine (45 μM) has cytotoxic effect and there is an inverse correlation between hydroethidine uptake and cell survival.³⁵

Since the early 1990's, fluorescence resulting from the oxidation of dihydroethidium (DHE) has been used as an O_2^- probe with success.²⁷ DHE has been established to detect O_2^- with end-product fluorescence measurement by many researchers.^{5,6,24,33,34,37} DHE fluorescence is inhibited by O_2^- scavengers such as superoxide dismutase (SOD) and nitric oxide (NO).²⁰ Products for the oxidation of DHE by O_2^- are well established. In the presence of O_2^- , DHE is oxidized to EOH and intermediate products. These intermediate products can react with $\cdot OH$ or H_2O_2 to form ethidium (E^+) to a much lesser extent. Whereas E^+ fluorescence is measured at excitation of 500–530 nm and emission of 590–620 nm, the EOH fluorescence is measured at an excitation and emission wavelength of 480 and 567 nm, respectively.^{8,33} EOH is stable within the cell, allowing for precise measurement of DHE fluorescence without risk of intra-conversion variability.

Fluorescence measurement of DHE yields O_2^- levels specific for either intracellular or extracellular locations.²² However, it is difficult to detect and quantify O_2^- because of its short life-time (a few seconds), low flux rate, fast self-dismutation rate, rapid reaction with multiple intra and extracellular scavengers such as SOD, vitamin C and E, glutathione (GSH) and NO,^{3,8} and fluorescent dye reacting with various species to form other products or intermediate products.^{10,21,35} For the detection of O_2^- using DHE fluorescence, HPLC, microplate reader analysis, and fluorometry have been proven effective for qualitative and quantitative measurement of O_2^- concentrations.¹⁶ However, the quantitative understanding of O_2^- interaction with DHE in experiments is needed. Without this, only qualitative measurement of O_2^- is possible. A quantitative measurement of O_2^- interaction will help us to further study the impact and mechanism of O_2^- resulting damage.

Several studies have focused on quantitative interaction of DHE with O_2^- .^{2,6,13,18,33,36} Laurindo *et al.*¹³ described the possible way to separate using HPLC and to quantify EOH, which is the main product of DHE and O_2^- interaction, and E^+ , which is the main

product of DHE and H_2O_2 interaction. Fink Bruno *et al.*⁶ reported that EOH formation is inhibited in the presence of SOD, which catalyzes O_2^- dismutation. After the addition of H_2O_2 , peroxyxynitrite ($ONOO^-$) or hypochlorous acid to O_2^- generation system of potassium superoxide and XOD, they reported no additional change in EOH formation. Benov *et al.*² showed that the ratio of E^+ formation/ O_2^- decreased as the flux of O_2^- increased. In addition, they showed that the DHE can catalyze the dismutation of O_2^- . Fernandes *et al.*⁵ showed that EOH increased after treatment of smooth muscle cells with AngII by detecting with HPLC and fluorescence micro-plate reader.

Zhao *et al.*³³ reported that the addition of DEA/NO (an NO donor) inhibits the EOH fluorescence in xanthine/XOD system. In addition, using competition kinetic analysis with SOD, they estimated a reaction rate constant for DHE and O_2^- interaction of $2.6 \pm 0.6 \times 10^5 M^{-1} s^{-1}$. Later, Zielonka *et al.*³⁶ used pulse radiolysis technique to calculate the rate constant between O_2^- and DHE is $2.0 \times 10^6 M^{-1} s^{-1}$. They also reported that DHE interaction with only O_2^- results in EOH formation.³⁴ Previous measurements of DHE interactions with O_2^- ignored the self-dismutation of O_2^- , which can lead to the overestimation of this reaction rate constant.

In this study, we systematically investigated interactions of O_2^- with DHE by measuring DHE and oxidized product EOH using XOD catalysis of HX oxidation to form O_2^- using a microplate reader. We varied enzyme (XOD), substrate (HX), and reactant (DHE) concentration over a wide range to understand how these can affect the DHE and O_2^- interaction. We also developed a biochemical kinetic model to quantify DHE and O_2^- interactions and to understand the effect of self-dismutation of O_2^- . As a result of this study, we provide a new reaction rate constant for the reaction between DHE and O_2^- .

MATERIALS AND METHODS

Materials

XOD, HX, catalase, ferricytochrome-c and phosphate buffer solution (PBS) were obtained from Sigma Chemical Co. (St. Louis, MO, USA). DHE was purchased from Invitrogen Corp. (Carlsbad, CA, USA).

O_2^- and DHE Reaction

Reactions were conducted in a 96-well Microtest™ Optilux™ Plate with a transparent bottom holding a total reagent volume of 250 μL in PBS (10 mM, pH 7.4). O_2^- was produced using HX and XOD enzyme

system.¹¹ Catalase was used to remove excess H_2O_2 , which is generated from the dismutation of O_2^- and the XOD/HX system. The reaction volume of 250 μL contained DHE, HX, catalase (100 U/mL) with or without XOD.

To understand the kinetics of the DHE and O_2^- reaction, we modified the kinetic analysis from an earlier study by Zhao *et al.*³³ that used the competition kinetic analysis to provide a rate constant of $2.6 \pm 0.6 \times 10^5 \text{ M}^{-1} \text{ s}^{-1}$ for the O_2^- and DHE reaction. Three sets of experiments were conducted. First, we varied XOD concentration 1, 1.5, 2.5, 5 mU/mL, and kept HX and DHE concentration constant at 0.25 mM and 5 μM , respectively. Second, we varied DHE concentration 2, 5, 10, 20, and 50 μM and kept HX and XOD concentration constant at 0.25 mM and 1.5 mU/mL, respectively. Finally, the HX concentration was varied to 0.0625, 0.125, and 0.25 mM and XOD and DHE concentration was kept at 1.5 mU/mL and 5 μM , respectively.

Fluorescence Measurement

In this study, EOH fluorescence was monitored by a Synergy 2 multi-detection microplate reader using a Gen5 microplate data collection & analysis software (BioTek Instruments Inc., VT, USA). As described by Zhao,³³ Robinson²⁴ and Laurindo¹³ the excitation/emission wavelength was chosen as 420/590 nm with a 50 nm or 35 nm slit width, respectively. The DHE fluorescence was measured at excitation/emission wavelength of 360/460 nm with a 40 nm slit width. The plate was read from 50% top, which was suitable for all these filters, and the sensitivity was set to be 70. The kinetic measurements were performed for 120 min and fluorescence was recorded every 3 min. The fluorescence values were obtained by subtracting the background fluorescence values obtained in PBS with HX, catalase and DHE in the absence of XOD.

To obtain the DHE concentration, we generated a standard curve of DHE (concentration vs. fluorescence) by measuring DHE fluorescence at DHE concentration of 1, 2, 5, 10, 20, and 50 μM in the same solution as experiment group without XOD. We observed that the DHE fluorescence without XOD in the solution (i.e., without superoxide) does not change significantly over 120 min.

O_2^- Production

O_2^- production was measured using a widely used rapid reduction of ferri-cytochrome c reduction assay.^{14,16} Absorbance readings at 550 nm were collected every min over 30 min. A molar extinction coefficient $21,000 \text{ M}^{-1} \text{ cm}^{-1}$ ³³ and a path length

0.975 cm were used to calculate O_2^- production of different HX and XOD concentration experiments. The absorbance assay volume was 250 μL in PBS with reagents including XOD (1, 1.5, 2.5, and 5 mU/mL), HX (0.0625, 0.125, and 0.25 mM), catalase (100 U/mL), and ferri-cytochrome c (81 μM). We determined the rate of O_2^- generation by multiplying the slope of ferri-cytochrome c generation with the reciprocal of extinction coefficient of ferri-cytochrome c and path length.

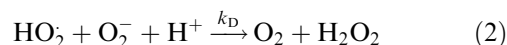
DHE and O_2^- Reaction Kinetic Analysis

We consider the following reactions occurring in the system to quantify the DHE and O_2^- interactions.

- i) Reaction between DHE and O_2^- yields a fluorescent product at a rate constant of k_{DHE} as follows:



- ii) We included the self-dismutation of O_2^- in the analysis. Earlier studies neglected this reaction.^{31,33} We also analyzed the effect of this reaction on the results of our study. In addition, we added large amount of catalase to scavenge H_2O_2 . The rate constant for self-dismutation of O_2^- (k_{D})^{1,23} is $8 \times 10^7 \text{ M}^{-1} \text{ s}^{-1}$ and the reaction occurs as follows:



Thus, the mass balance equation in the reaction system for the species of interests, O_2^- , and DHE, can be written as:

$$\frac{dC_{\text{O}_2^-}}{dt} = S_{\text{O}_2^-} - k_{\text{DHE}} C_{\text{DHE}} C_{\text{O}_2^-} - k_{\text{D}} C_{\text{HO}_2} C_{\text{O}_2^-}, \quad (3)$$

$$\frac{dC_{\text{DHE}}}{dt} = -k_{\text{DHE}} C_{\text{DHE}} C_{\text{O}_2^-} \quad (4)$$

Note that (i) $S_{\text{O}_2^-}$ is the rate of O_2^- production in the system and was obtained from ferri-cytochrome c reduction assay as described in the previous subsection, and (ii) the rate of O_2^- dismutation can be simplified assuming a rapid equilibrium of HO_2/O_2^- with $C_{\text{HO}_2}/C_{\text{O}_2^-} = 0.0025$, which is based on $\text{pK}_a = 4.8$ and the pH value of 7.4 and the relationship for the mole fraction of HO_2 ($f = \frac{1}{1+10^{(\text{pK}_a-\text{pH})}}$). We assumed initial concentration of O_2^- is zero.

For a given experimental condition, Eqs. (3) and (4) were solved using the MatLab® with initial concentrations of DHE (varied) and O_2^- . We fitted the experimental data of DHE concentration (measured at ex/em of 360/460 nm) with the model predictions by

varying k_{DHE} . As shown in Eq. (5), we used least square estimation and minimized the sum of squares of error to obtain the rate constant, k_{DHE} .

$$Q = \sum_{j=1}^k \sum_{i=1}^k (y_{\text{exp}} - y_{\text{model}})^2 \quad (5)$$

where y_{exp} and y_{model} are the average measured and model predicted DHE concentration values, respectively for one experiment condition. For each of the three sets of experiments mentioned earlier, k represents the number of varying conditions in one set of experiments and n represents the number of time data points in one experimental conditions. We fit the data only for first 18 min of experiments, therefore n is equal to 7. For each set of experiments, a new value of Q was calculated. The reported rate constant in this manuscript corresponds to the minimum Q .

Statistical Analysis

Three runs were performed for each experimental condition and all values are reported as mean \pm SE. We used the Matlab function ode 15 s to solve the simultaneous differential equations and used absolute error and relative error of 1×10^{-13} . For optimization of k_{DHE} , we used fminsearch function with a toleration error for Q of 1×10^{-13} .

RESULTS

DHE Concentration Related Change in DHE and EOH Fluorescence

Figures 1a and 1b show the reduction of DHE fluorescence and the accumulation of EOH fluorescence for DHE concentration of 2, 5, 10, 20, and 50 μM over 120 min. The initial XOD and HX concentration was 1.5 mU/mL and 0.25 mM, respectively. Both DHE and EOH fluorescence had two phases of fluorescence change. The fluorescence changed at an initial high slope followed by a small slope. The DHE fluorescence decreased linearly for the first 20 min for all DHE concentrations. In addition, an initial faster decrease in DHE fluorescence and increase in EOH fluorescence was observed at higher DHE concentrations ($\geq 10 \mu\text{M}$). After 40 min, DHE reacted completely and the formation of EOH reached a plateau except for the DHE concentration of 20 and 50 μM .

Enzyme XOD Concentration Related Change in DHE and EOH Fluorescence

Figures 2a and 2b show DHE and EOH fluorescence for XOD concentration of 1, 1.5, 2.5, and 5 mU/mL over 120 min. The initial DHE and HX concentration

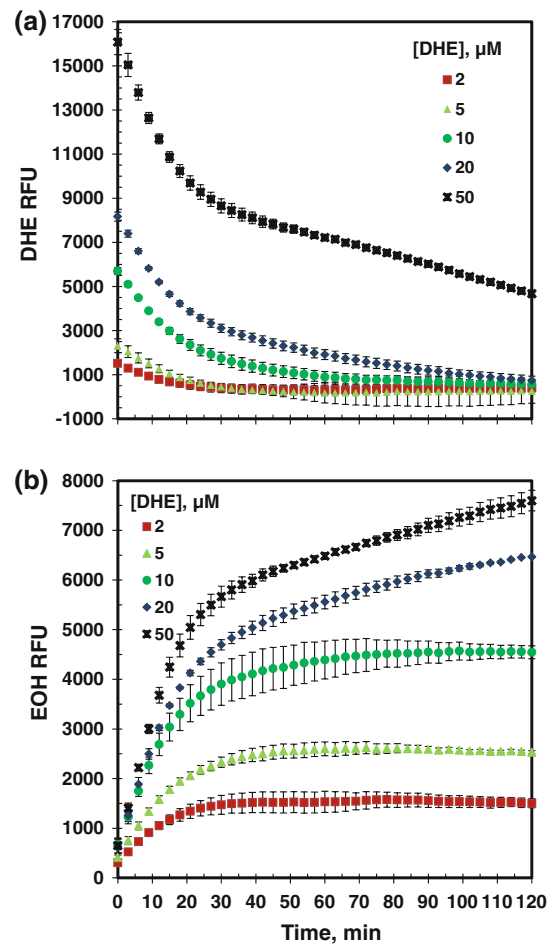


FIGURE 1. Measured DHE and EOH fluorescence as a function of DHE concentration. (a) and (b) The DHE and EOH fluorescence with respect to time for DHE concentration of 2, 5, 10, 20, and 50 μM with XOD concentration of 1.5 mU/mL and HX concentration of 0.25 mM for 120 min.

was 5 μM and 0.25 mM, respectively. The DHE and EOH fluorescence again show the two phases for changes of fluorescence density; an initial steep change for the first 20 min followed by a slow change. In addition, Figs. 2a and 2b show that the higher the XOD concentration, the faster the initial decrease in DHE fluorescence and the increase in EOH fluorescence. At XOD concentration of 1 mU/mL, Fig. 2b shows that the DHE did not completely transform into EOH as demonstrated by non-convergence of RFU at 120 min with other XOD concentrations. This may be possible because of auto-oxidation of DHE resulting in other products and not EOH or sufficient superoxide formation to react with DHE.

Substrate HX Concentration Related Change in DHE and EOH Fluorescence

Figures 3a and 3b show the effect of HX concentration of 0.0625, 0.125, and 0.25 mM on DHE and

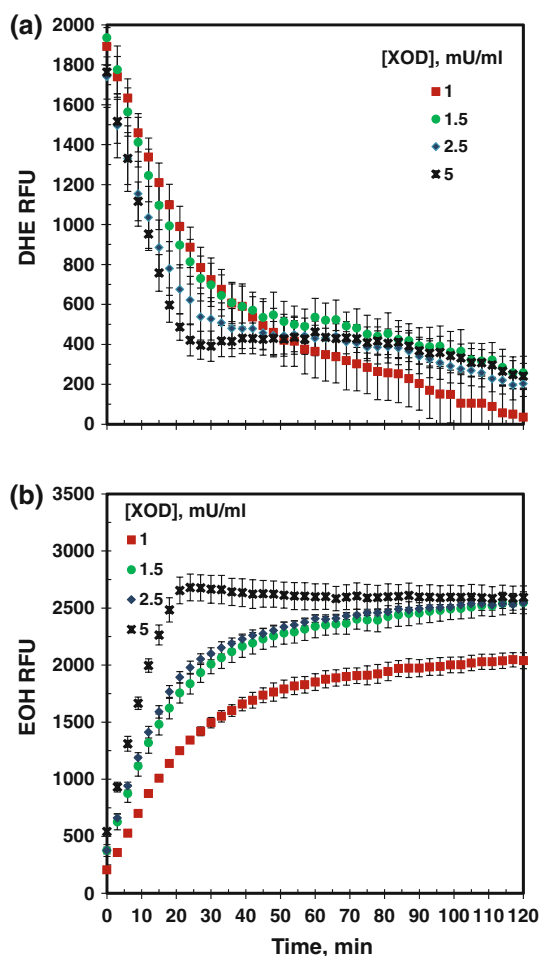


FIGURE 2. Measured DHE and EOH fluorescence as a function of XOD concentration. (a) and (b) shows the DHE and EOH fluorescence for XOD concentration of 1.0, 1.5, 2.5 and 5 mU/mL for HX (=0.25 mM) and DHE (=5 μ M) for 120 min.

EOH fluorescence, respectively. The initial DHE concentration was 5 μ M and 1.5 mU/mL for XOD. The same two phases in DHE and EOH fluorescence were also present in this set of experiment. However, the initial DHE and EOH fluorescence changes were higher at increased HX concentrations. Figure 3b also shows that DHE did not completely convert into EOH at HX concentration of 0.0625 and 0.125 mM as compared with HX concentration of 0.25 mM.

Absorbance Measurements of O_2^- Generation (Product of XOD and HX)

Figures 4a and 4b describe ferrocyanochrome c absorbance for the measurement of O_2^- formation rate as a function of XOD concentration and HX concentration, respectively. These data is required for the kinetic analysis. As shown, the ferrocyanochrome c absorbance increased linearly with varying slope for the first 20 min for all conditions. It implies that O_2^-

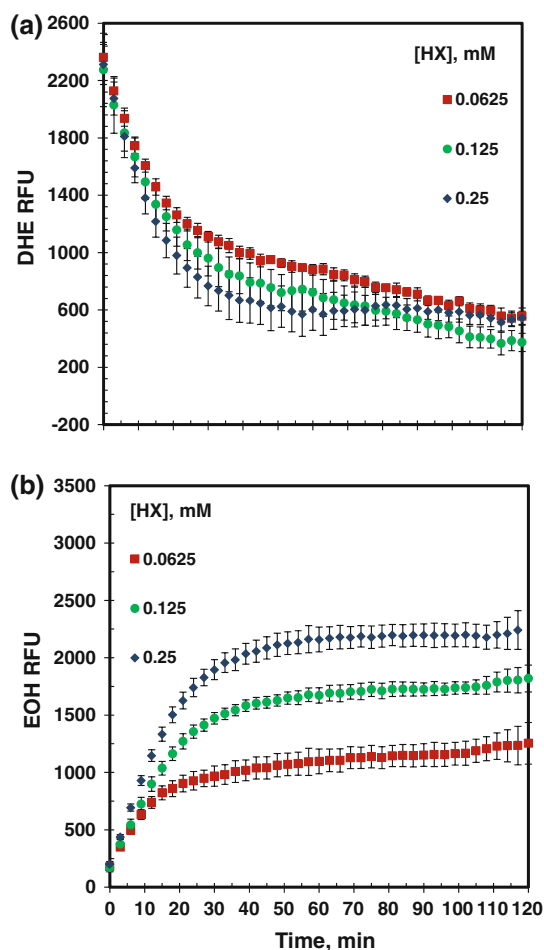


FIGURE 3. Measured DHE and EOH fluorescence as a function of HX concentration. (a) and (b) shows the DHE and EOH fluorescence for HX concentration of 0.0625, 0.125 and 0.25 mM with XOD (=1.5 mU/mL) and DHE (=5 μ M) for 120 min.

formation rate is constant for a given condition over the first 20 min. For a given HX and XOD concentration, the O_2^- formation rate was calculated by multiplying the slope of increase in ferrocyanochrome c absorbance with the reciprocal of EC value ($21 \text{ mM}^{-1} \text{ cm}^{-1}$) and path length (0.975 cm). At 1, 1.5, 2.5, and 5 mU/mL XOD concentration, the O_2^- formation rate was 0.943, 1.465, 1.636, and 2.623 μ M/min, respectively. The O_2^- formation rate was 0.866, 1.189, and 1.473 μ M/min at 0.0625, 0.125, and 0.25 mM HX concentration. This data indicated the higher substrate and enzyme concentration leads to the higher O_2^- formation rate.

Standard Curve of DHE Fluorescence vs. Concentration

As shown in Fig. 5, we generated the standard curve of DHE fluorescence vs. DHE concentration by fitting DHE concentrations (1, 2, 5, 10, 20, and 50 μ M) with their corresponding initial fluorescence. As we used a

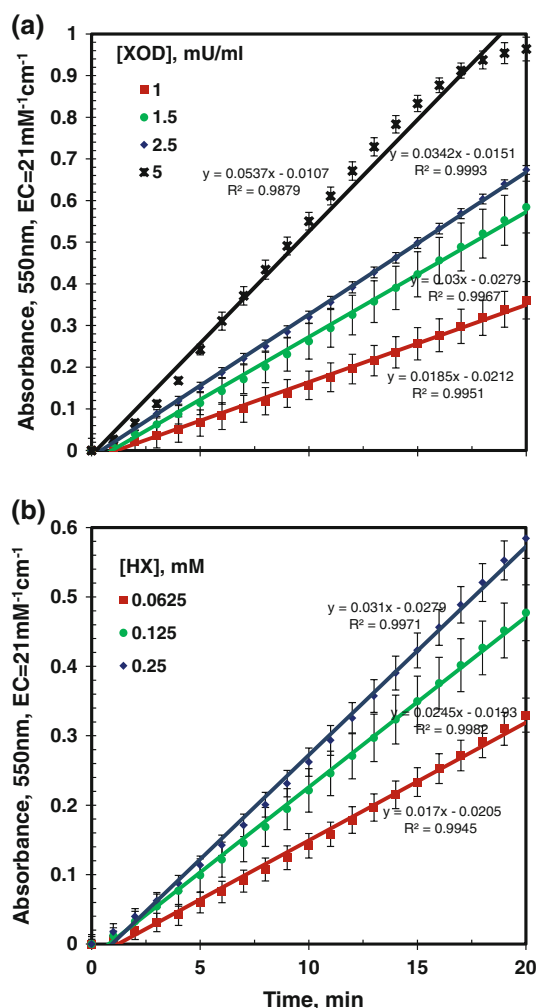


FIGURE 4. O_2^- generation rate by HX-XOD system determined by measuring ferrocyanochrome c at 550 nm ($EC = 21 \text{ mM}^{-1} \text{ cm}^{-1}$). (a) The absorbance of ferrocyanochrome c for XOD concentration of 1.0, 1.5, 2.5 and 5 mU/mL for HX (=0.25 mM). (b) The absorbance of ferrocyanochrome c for HX concentration of 0.0625, 0.125 and 0.25 mM with XOD (=1.5 mU/mL).

very wide range of DHE concentration, the optimal fit was not linear. However, the nonlinear relationship ($R^2 = 0.9965$) between DHE concentration and RFU is $[DHE], \mu\text{M} = 1 \times 10^{-7} \times (\text{DHE RFU})^2 + 0.0014 \times (\text{DHE RFU})$.

Kinetic Analysis of DHE and O_2^- Reaction

In order to obtain the kinetic rate constant, we fitted measured experimental data with model data by varying k_{DHE} . We used non-linear relationships from previous section to convert DHE RFU into DHE concentration.

First, we fitted experimental data from Fig. 1a with varying DHE concentration and the constant O_2^- formation rate of $1.469 \mu\text{M}/\text{min}$, which is the average value

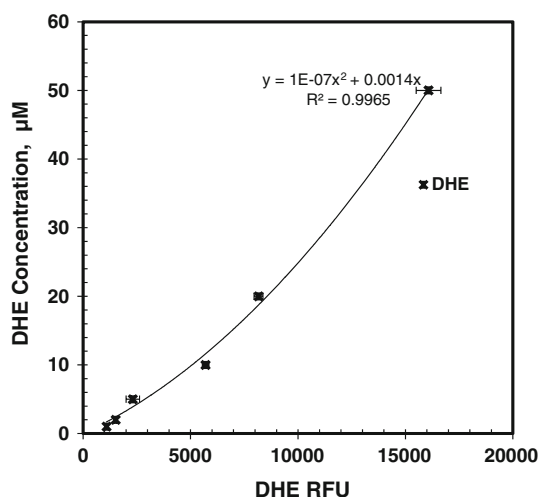


FIGURE 5. Standard curve of DHE concentration vs. DHE fluorescence. This figure shows DHE relative fluorescence unit (RFU) vs. DHE concentration for standard curve.

of 1.465 and $1.473 \mu\text{M}/\text{min}$ based on the ferrocyanochrome c absorbance data at $XOD = 1.5 \text{ mU}/\text{mL}$ and $HX = 0.25 \text{ mM}$. The minimum sum of squares of error between experimental data and predicted model data (Q) was $4.045 \times 10^3 \text{ M}^{-1} \text{ s}^{-1}$. The minimum Q was obtained with a reaction rate constant of DHE and O_2^- of $2.116 \times 10^3 \text{ M}^{-1} \text{ s}^{-1}$. The resulting fit with experimental data is shown in Fig. 6a. As seen, the model data closely predicted each point of experimental data for 18 min for all DHE concentrations.

Next, we fitted experimental data from Figs. 2a and 3a for varying XOD concentration and HX concentration, respectively. These conditions resulted in varying O_2^- formation rates as described in previous sections for ferrocyanochrome c absorbance data. Using different O_2^- formation rates, we obtained k_{DHE} for each of the XOD and HX concentration variation. The resulting fit with experimental data is shown in Figs. 6b and 6c. At 1, 1.5, 2.5, and 5 mU/mL XOD concentration, the k_{DHE} is 1.933×10^3 , 1.827×10^3 , 2.626×10^3 , and $2.372 \times 10^3 \text{ M}^{-1} \text{ s}^{-1}$, and at the HX concentration of 0.0625, 0.125, and 0.25 mM, the k_{DHE} reaction is 2.191×10^3 , 2.208×10^3 , and $2.295 \times 10^3 \text{ M}^{-1} \text{ s}^{-1}$ resulted in the best fit between experimental and predicted data. The respective Q value was 5.436×10^{-15} , 2.415×10^{-14} , 1.447×10^{-13} , 7.072×10^{-15} , 7.327×10^{-15} , 4.122×10^{-15} , and 2.628×10^{-15} . Based on all these reaction rate constant of DHE and O_2^- , the mean rate of reaction of DHE with O_2^- , k_{DHE} , is $2.169 \pm 0.059 \times 10^3 \text{ M}^{-1} \text{ s}^{-1}$.

DISCUSSION

O_2^- is the precursor of many derivative ROS, and can rapidly react with NO to inactivate NO

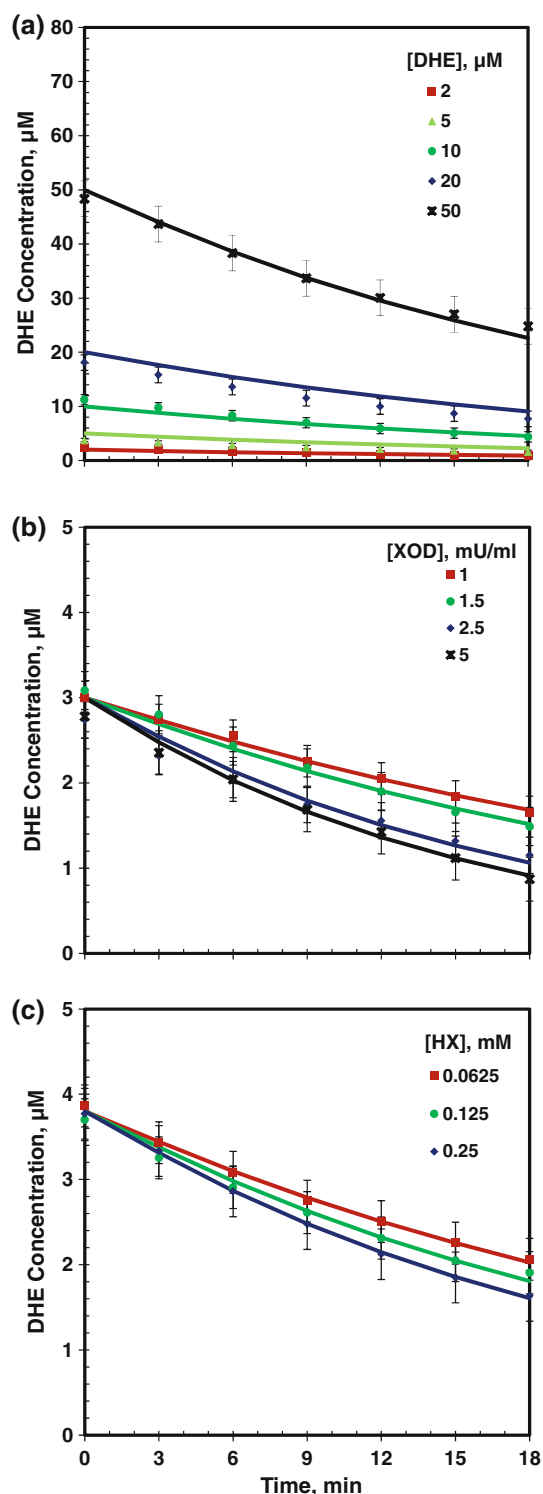


FIGURE 6. Measured and predicted DHE concentration profiles using kinetic analysis. (a)–(c) The kinetic model results (solid lines) for experimental data (discrete symbols) of varying DHE concentration, XOD concentration and HX concentrations, respectively.

bioavailability and augment production of RNS. Therefore, the quantitative measurement of O_2^- measurement is critical. Traditionally, the fluorescence

product of DHE was measured at the excitation/emission wavelength of 510/595 nm, which is the wavelength for detecting E^+ . The reaction of O_2^- and DHE also generates EOH that is confirmed to be the specific products formed. Researchers have started using excitation/emission wavelength to detect EOH fluorescence at either sensitive or specific wavelengths of 480/580 nm and 396/579 nm, respectively.^{5,13,24,33} In this study, we have confirmed that DHE fluorescence can be used to quantify O_2^- by HX-XOD system using microplate readers like other methods of O_2^- measurement.^{8,13,30,32,33} The development of mathematical model for DHE interaction with O_2^- is novel and can be extended further for understanding many aspects of oxidative stress interactions including NO at molecular level. In addition, we provide a calibration curve for DHE concentration using RFU for the first time. We propose a DHE and O_2^- reaction rate constant of $2.169 \pm 0.059 \times 10^3 \text{ M}^{-1} \text{ s}^{-1}$.

O_2^- Measurements

A predictable cell-free O_2^- generating system was utilized to achieve measurements of O_2^- concentration using a common fluorescence detection method and microplate reader analysis. The formation of EOH and depletion of DHE was specific to O_2^- as seen in Fig. 1 with varying DHE concentration. The change in the rate of DHE fluorescence was dependent on O_2^- formation from the HX-XOD system as seen in Figs. 2 and 3. However, in the absence of O_2^- , DHE depletion was also influenced by autooxidation of DHE at later time points (>40 min). Both the increase in EOH and the decrease in DHE occurred in two linear phases: a steep initial change followed by a slower, steadier change. As the DHE concentration or the rate of O_2^- formation increased through the increase in the concentration of HX and XOD, both the decrease in DHE fluorescence and increase in EOH fluorescence would be accelerated. From these profiles, we showed that the higher the concentration of reactant, the faster the reaction between DHE and O_2^- . The biphasic curve in Figs. 1, 2, 3 was because of the change in the superoxide production rate at later time points that were seen after 30 min in most cases (data not shown) during absorbance assay (Fig. 4). We showed that using a wide ranging superoxide production rate (varying HX and XOD concentrations for the first 18 min), we were able to fit the data with the k_{DHE} .

Currently, much research begins to pay attention to the accuracy of fluorescence detection of DHE- O_2^- reaction.^{13,35} These studies suggest that HPLC analysis is a reliable method for measurement of DHE detection of O_2^- . Due to the extremely short O_2^- half-life and rapid dismutation reaction rate, DHE fluorescence

detection is prone to underestimation of actual O_2^- production.^{34,37} Additionally, studies have shown that DHE can react with various oxidants found within the cell, including mitochondrial cytochrome hemes, hypochlorous acid, myeloperoxidase, horseradish peroxidase $ONOO^-$, OH , H_2O_2 , compounds I and II, Fenton reagent, and so on.^{10,19,21,35} Shao *et al.*²⁸ also demonstrated that certain potent diet antioxidants can greatly decrease O_2^- concentration even in extreme acute oxidative stress. The total O_2^- production measurements are impossible as reported.⁸ At best, it will be an estimate due to the varying amount of O_2^- consumption among various interactions with other species.

However, Munzel¹⁷ has suggested that it is wise to use two or more techniques to detect O_2^- . Reliable conclusions could be drawn from similar results by using different measurements. In this study, we used cytochrome c absorbance and DHE fluorescence to detect O_2^- generation. Our results show that the formed products between superoxide and DHE or Cyt c respectively increase linearly. Moreover, by fitting our experimental data with computational model, we confirmed that DHE fluorescence measurement and microplate reader analysis can describe as a quantitative measurement of localized O_2^- concentration *in vivo*, which will provide us an effective method to detect O_2^- .

DHE- O_2^- Reaction Rate Constant of $2.169 \pm 0.059 \times 10^3 M^{-1} s^{-1}$

Based on experimental measurements and computational modeling in this study, we report a reaction rate constant of $\sim 2.169 \pm 0.059 \times 10^3 M^{-1} s^{-1}$, which is $\sim 100\times$ lower than the previously reported value of $2.6 \pm 0.6 \times 10^5 M^{-1} s^{-1}$.³³ There are two possible reasons for this discrepancy. Firstly, the kinetic analysis in our study is more detailed with respect to the reactions occurring in the system. Secondly, the self-dismutation of O_2^- was considered in present study that increased O_2^- consumption and was not considered in previous study. The rate constant of O_2^- self-dismutation ($8.0 \times 10^7 M^{-1} s^{-1}$) is lower than that of O_2^- and SOD reaction ($1.6 \times 10^9 M^{-1} s^{-1}$),²³ but higher than that of DHE and O_2^- reaction ($2.169 \pm 0.059 \times 10^3 M^{-1} s^{-1}$). Therefore, it is necessary to include O_2^- self-dismutation in DHE and O_2^- reaction system as done in this study.

We analyzed reasons behind a lower reaction rate constant for DHE reaction with O_2^- . We simulated the experiment performed by Zhao *et al.*³³ for k_{DHE} of 2.17×10^3 and $2.69 \times 10^5 M^{-1} s^{-1}$ ³³ with and without the inclusion of self-dismutation of O_2^- . We used a $50 \mu M$ initial DHE and $8 \mu M/min$ O_2^- generation

rate,³³ and the results are plotted in Fig. 7. Figures 7a and 7b show results for k_{DHE} of $2.69 \times 10^5 M^{-1} s^{-1}$ without and with the inclusion of self-dismutation of O_2^- , respectively, while Figs. 7c and 7d show results for k_{DHE} of $2.17 \times 10^3 M^{-1} s^{-1}$ without and with the inclusion of self-dismutation of O_2^- , respectively. Figures 7a, 7b, and 7c are similar to each other and show that DHE is completely consumed and transformed to EOH at 6, 7, and 8 min respectively. However, as Zhao *et al.*³³ described that the intensity of product fluorescence linearly increased (Figure 10 in Ref.³³) and kept the same trend for first 20 min until they added DEA/NO into this reaction buffer. The model simulation results are not in agreement with experimental results. Therefore, we can conclude that DHE would fast consume for both k_{DHE} when self-dismutation of O_2^- is neglected.

However, when we include self-dismutation with the lower k_{DHE} , Fig. 7d shows that there is an initial linear increase in EOH and decrease in DHE for the first 20 min followed by a slow change in EOH and DHE. In addition, we also simulated the experimental results of the current study without (Fig. 7e) or with (Fig. 7f) self-dismutation reaction at $5 \mu M$ DHE and $1.465 \mu M/min$ superoxide production rate HX ($0.25 mM$) and XOD ($1.5 mU/mL$). As shown in Fig. 7e, the depletion of DHE occurred in the first 10 min without self-dismutation reaction. Figure 7f shows that the model predictions with self-dismutation reaction are similar to the experiment result i.e., DHE can last much longer. This indicated that O_2^- self-dismutation cannot be neglected and model results are in agreement with experimental results.

Implications of Slower Reaction Rate of DHE with O_2^-

A slower reaction rate of DHE with O_2^- is more reasonable for O_2^- measurements. In addition to superoxide production rate, the most important factors for the determination of O_2^- concentration in a given system are SOD and NO. SOD can fast dismutate O_2^- into H_2O_2 and NO can quickly react with O_2^- to generate RNS. The slower reaction rate of DHE- O_2^- implies that the presence of DHE does not affect O_2^- concentration, whereas the faster reaction rate implies that DHE competes with SOD and NO for O_2^- and reduces O_2^- concentration. Therefore, the respective changes in DHE fluorescence indicate change in O_2^- concentration in the system for the slower reaction rate. Many other chemical reactions simultaneously occur in the physiological system, the results from this study can be extrapolated to explain the effect of these reactions on oxidative stress. The change in DHE fluorescence will be in the same trend as these other reactions affect the O_2^- concentration. Thus, the

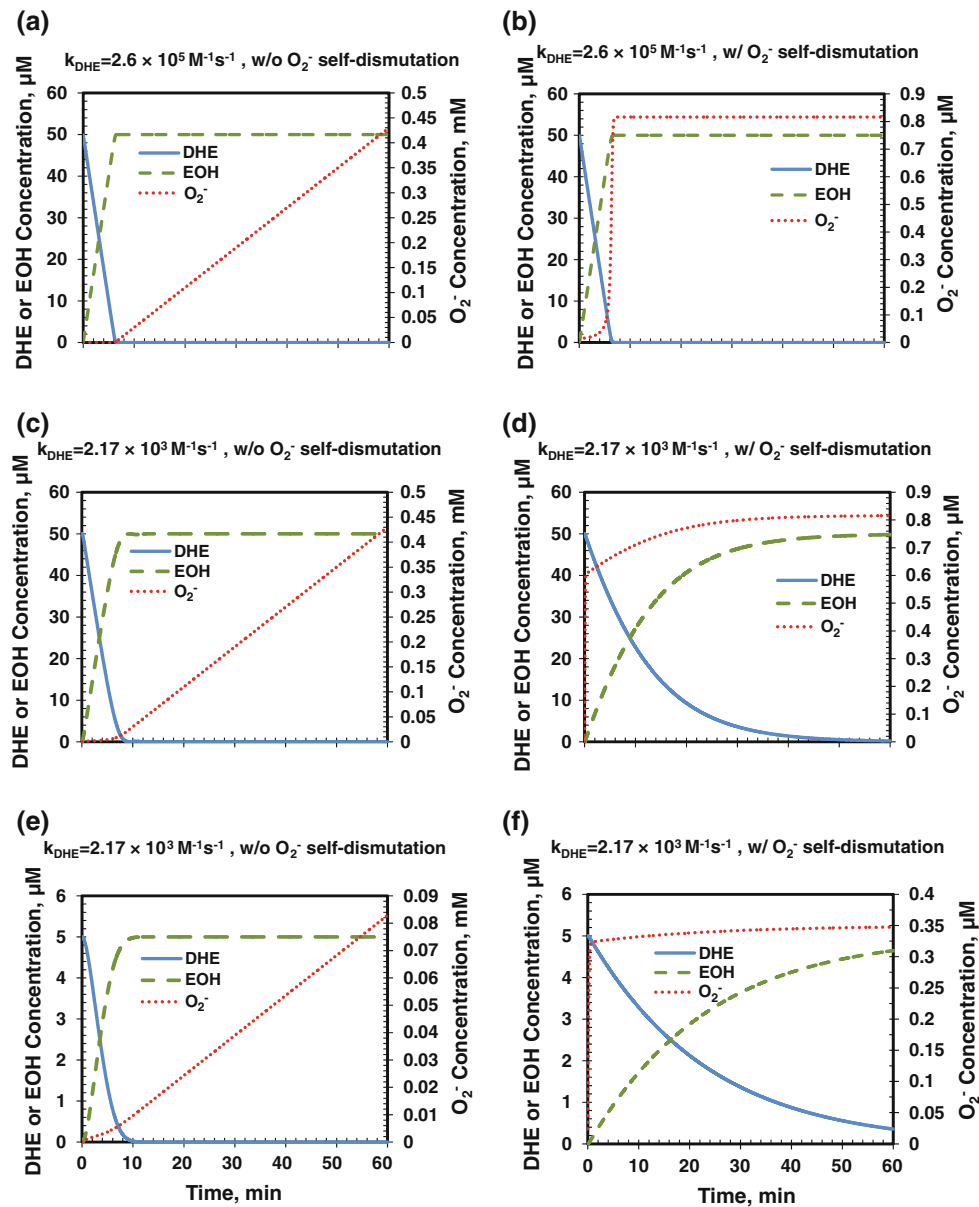


FIGURE 7. Predicted O_2^- , EOH, and DHE concentration profiles using kinetic analysis. This figure shows the predicted concentration profiles from the kinetic model for DHE and O_2^- reaction for 120 min. DHE and EOH concentration are shown on left axis. O_2^- concentration is shown on right axis. (a)–(d) DHE and O_2^- reaction under O_2^- formation of $8 \mu\text{M}/\text{min}$ and DHE of $50 \mu\text{M}$, and (e), (f) shows DHE and O_2^- reaction under O_2^- formation of $1.465 \mu\text{M}/\text{min}$ and DHE of $5 \mu\text{M}$. (a) and (b) The profile for without and with O_2^- self-dismutation, respectively for $2.6 \times 10^5 \text{ M}^{-1} \text{ s}^{-1}$ reaction rate constant of DHE and O_2^- reaction. (c) and (e) The profile for without O_2^- self-dismutation for $2.17 \times 10^3 \text{ M}^{-1} \text{ s}^{-1}$ reaction rate constant of DHE and O_2^- reaction. (d) and (f) shows the profile for with O_2^- self-dismutation for $2.17 \times 10^3 \text{ M}^{-1} \text{ s}^{-1}$ reaction rate constant of DHE and O_2^- reaction.

fluorescence probes designed to exhibit a relatively low rate constant with the analyte detected will be ideal *in vivo* detection of O_2^- . In ROS and RNS mathematical modeling, SOD can fast dismutate O_2^- into H_2O_2 and NO can quickly react with O_2^- to generate RNS. We conclude that DHE can be used to detect the O_2^- concentration without the interference of pathways in the cell system. It will be useful to determine the accumulated O_2^- concentrations and to predict damages in cell systems.

In conclusion, an accurate method for O_2^- measurement would be highly beneficial to the potential diagnosis and treatment of a number of different biological issues. This current study describes some necessary considerations for experimental measurement and analysis of O_2^- concentrations. DHE measurement of O_2^- may provide a more accurate description of oxidative stress, especially for O_2^- . This detailed kinetic analysis study provided a DHE and O_2^- reaction rate constant of $\sim 2.169 \pm 0.059 \times 10^3 \text{ M}^{-1} \text{ s}^{-1}$

that is $\sim 100\times$ lower than the previously reported value of $2.6 \pm 0.6 \times 10^5 \text{ M}^{-1} \text{ s}^{-1}$, and is more appropriate for DHE O_2^- measurement.

ACKNOWLEDGMENTS

This study was supported by NIH grant # R01 HL084337.

REFERENCES

- ¹Behar, D., G. Czapski, J. Rabani, L. M. Dorfman, and H. A. Schwarz. Acid dissociation constant and decay kinetics of perhydroxyl radical. *J. Phys. Chem-US*. 74:3209, 1970.
- ²Benov, L., L. Szejnberg, and I. Fridovich. Critical evaluation of the use of hydroethidine as a measure of superoxide anion radical. *Free Radic. Biol. Med.* 25:826–831, 1998.
- ³Deng, T., K. Xu, L. Zhang, and X. Zheng. Dynamic determination of Ox-LDL-induced oxidative/nitrosative stress in single macrophage by using fluorescent probes. *Cell Biol. Int.* 32:1425–1432, 2008.
- ⁴Droge, W. Free radicals in the physiological control of cell function. *Physiol. Rev.* 82:47–95, 2002.
- ⁵Fernandes, D. C., J. Wosniak, Jr., L. A. Pescatore, M. A. Bertoline, M. Liberman, F. R. Laurindo, and C. X. Santos. Analysis of DHE-derived oxidation products by HPLC in the assessment of superoxide production and NADPH oxidase activity in vascular systems. *Am. J. Physiol. Cell Physiol.* 292:C413–C422, 2007.
- ⁶Fink, B., K. Laude, L. McCann, A. Doughan, D. G. Harrison, and S. Dikalov. Detection of intracellular superoxide formation in endothelial cells and intact tissues using dihydroethidium and an HPLC-based assay. *Am. J. Physiol. Cell Physiol.* 287:C895–C902, 2004.
- ⁷Fujita, M., R. Tsuruta, S. Kasaoka, K. Fujimoto, R. Tanaka, Y. Oda, M. Nanba, M. Igarashi, M. Yuasa, T. Yoshikawa, and T. Maekawa. In vivo real-time measurement of superoxide anion radical with a novel electrochemical sensor. *Free Radic. Biol. Med.* 47:1039–1048, 2009.
- ⁸Georgiou, C. D., I. Papapostolou, N. Patsoukis, T. Tsegenidis, and T. Sideris. An ultrasensitive fluorescent assay for the in vivo quantification of superoxide radical in organisms. *Anal. Biochem.* 347:144–151, 2005.
- ⁹Hernandes, M. S., L. R. Britto, C. C. Real, D. O. Martins, and L. R. Lopes. Reactive oxygen species and the structural remodeling of the visual system after ocular enucleation. *Neuroscience* 170:1249–1260, 2010.
- ¹⁰Kalyanaraman, B., V. Darley-Usmar, K. J. A. Davies, P. A. Dennery, H. J. Forman, M. B. Grisham, G. E. Mann, K. Moore, L. J. Roberts, and H. Ischiropoulos. Measuring reactive oxygen and nitrogen species with fluorescent probes: challenges and limitations. *Free Radic. Biol. Med.* 52:1–6, 2012.
- ¹¹Kavdia, M., J. L. Stanfield, and R. S. Lewis. Nitric oxide, superoxide, and peroxynitrite effects on the insulin secretion and viability of betaTC3 cells. *Ann. Biomed. Eng.* 28:102–109, 2000.
- ¹²Kishida, K. T., and E. Klann. Sources and targets of reactive oxygen species in synaptic plasticity and memory. *Antioxid. Redox Signal.* 9:233–244, 2007.
- ¹³Laurindo, F. R., D. C. Fernandes, and C. X. Santos. Assessment of superoxide production and NADPH oxidase activity by HPLC analysis of dihydroethidium oxidation products. *Methods Enzymol.* 441:237–260, 2008.
- ¹⁴Massey, V. The microestimation of succinate and the extinction coefficient of cytochrome c. *Biochim. Biophys. Acta* 34:255–256, 1959.
- ¹⁵McFarland, R., A. Blokhin, J. Sydnor, J. Mariani, and M. W. Vogel. Oxidative stress, nitric oxide, and the mechanisms of cell death in Lurcher Purkinje cells. *Dev. Neurobiol.* 67:1032–1046, 2007.
- ¹⁶Messner, K. R., and J. A. Imlay. In vitro quantitation of biological superoxide and hydrogen peroxide generation. *Methods Enzymol.* 349:354–361, 2002.
- ¹⁷Munzel, T., I. B. Afanas'ev, A. L. Kleschyov, and D. G. Harrison. Detection of superoxide in vascular tissue. *Arterioscler. Thromb. Vasc. Biol.* 22:1761–1768, 2002.
- ¹⁸Papaharalambus, C. A., and K. K. Griendling. Basic mechanisms of oxidative stress and reactive oxygen species in cardiovascular injury. *Trends Cardiovasc. Med.* 17:48–54, 2007.
- ¹⁹Papapostolou, I., N. Patsoukis, and C. D. Georgiou. The fluorescence detection of superoxide radical using hydroethidine could be complicated by the presence of heme proteins. *Anal. Biochem.* 332:290–298, 2004.
- ²⁰Paravicini, T. M., and R. M. Touyz. NADPH oxidases, reactive oxygen species, and hypertension: clinical implications and therapeutic possibilities. *Diabetes Care* 31(Suppl 2):170–180, 2008.
- ²¹Patsoukis, N., I. Papapostolou, and C. D. Georgiou. Interference of non-specific peroxidases in the fluorescence detection of superoxide radical by hydroethidine oxidation: a new assay for H_2O_2 . *Anal. Bioanal. Chem.* 381:1065–1072, 2005.
- ²²Peshavariya, H. M., G. J. Dusting, and S. Selemidis. Analysis of dihydroethidium fluorescence for the detection of intracellular and extracellular superoxide produced by NADPH oxidase. *Free Radic. Res.* 41:699–712, 2007.
- ²³Potdar, S., and M. Kavdia. NO/peroxynitrite dynamics of high glucose-exposed HUVECs: chemiluminescent measurement and computational model. *Microvasc. Res.* 78:191–198, 2009.
- ²⁴Robinson, K. M., M. S. Janes, M. Pehar, J. S. Monette, M. F. Ross, T. M. Hagen, M. P. Murphy, and J. S. Beckman. Selective fluorescent imaging of superoxide in vivo using ethidium-based probes. *Proc. Natl. Acad. Sci. U. S. A.* 103:15038–15043, 2006.
- ²⁵Rojas, A., H. Figueroa, L. Re, and M. A. Morales. Oxidative stress at the vascular wall. Mechanistic and pharmacological aspects. *Arch. Med. Res.* 37:436–448, 2006.
- ²⁶Ryter, S. W., H. P. Kim, A. Hoetzel, J. W. Park, K. Nakahira, X. Wang, and A. M. Choi. Mechanisms of cell death in oxidative stress. *Antioxid. Redox Signal.* 9:49–89, 2007.
- ²⁷Selemidis, S., G. J. Dusting, H. Peshavariya, B. K. Kemp-Harper, and G. R. Drummond. Nitric oxide suppresses NADPH oxidase-dependent superoxide production by S-nitrosylation in human endothelial cells. *Cardiovasc. Res.* 75:349–358, 2007.
- ²⁸Shao, Z. H., J. T. Xie, T. L. Vanden Hoek, S. Mehendale, H. Aung, C. Q. Li, Y. Qin, P. T. Schumacker, L. B. Becker, and C. S. Yuan. Antioxidant effects of American ginseng

- berry extract in cardiomyocytes exposed to acute oxidant stress. *Biochim. Biophys. Acta* 1670:165–171, 2004.
- ²⁹Tarpey, M. M., C. R. White, E. Suarez, G. Richardson, R. Radi, and B. A. Freeman. Chemiluminescent detection of oxidants in vascular tissue. Lucigenin but not coelenterazine enhances superoxide formation. *Circ. Res.* 84:1203–1211, 1999.
- ³⁰Tarpey, M. M., D. A. Wink, and M. B. Grisham. Methods for detection of reactive metabolites of oxygen and nitrogen: in vitro and in vivo considerations. *Am. J. Physiol. Regul. Integr. Comp. Physiol.* 286:R431–R444, 2004.
- ³¹Vasquez-Vivar, J., J. Whitsett, P. Martasek, N. Hogg, and B. Kalyanaraman. Reaction of tetrahydrobiopterin with superoxide: EPR-kinetic analysis and characterization of the pteridine radical. *Free Radic. Biol. Med.* 31:975–985, 2001.
- ³²Wardman, P. Fluorescent and luminescent probes for measurement of oxidative and nitrosative species in cells and tissues: progress, pitfalls, and prospects. *Free Radic. Biol. Med.* 43:995–1022, 2007.
- ³³Zhao, H., S. Kalivendi, H. Zhang, J. Joseph, K. Nithipatikom, J. Vasquez-Vivar, and B. Kalyanaraman. Superoxide reacts with hydroethidine but forms a fluorescent product that is distinctly different from ethidium: potential implications in intracellular fluorescence detection of superoxide. *Free Radic. Biol. Med.* 34:1359–1368, 2003.
- ³⁴Zielonka, J., M. Hardy, and B. Kalyanaraman. HPLC study of oxidation products of hydroethidine in chemical and biological systems: ramifications in superoxide measurements. *Free Radic. Biol. Med.* 46:329–338, 2009.
- ³⁵Zielonka, J., and B. Kalyanaraman. Hydroethidine- and MitoSOX-derived red fluorescence is not a reliable indicator of intracellular superoxide formation: another inconvenient truth. *Free Radic. Biol. Med.* 48:983–1001, 2010.
- ³⁶Zielonka, J., T. Sarna, J. E. Roberts, J. F. Wishart, and B. Kalyanaraman. Pulse radiolysis and steady-state analyses of the reaction between hydroethidine and superoxide and other oxidants. *Arch. Biochem. Biophys.* 456:39–47, 2006.
- ³⁷Zielonka, J., J. Vasquez-Vivar, and B. Kalyanaraman. Detection of 2-hydroxyethidium in cellular systems: a unique marker product of superoxide and hydroethidine. *Nat. Protoc.* 3:8–21, 2008.